Dispersion Management for Atomic Matter Waves

B. Eiermann,[1] P. Treutlein,[1,2] Th. Anker,[1] M. Albiez,[1] M. Taglieber,[1] K.-P. Marzlin,[1] and M. K. Oberthaler[1]

[1]*Fachbereich Physik, Universität Konstanz, Fach M696, 78457 Konstanz, Germany*

[2]*Sektion Physik, Ludwig-Maximilians-Universität, Schellingstrasse 4, 80799 München, Germany*

(Received 14 March 2003; published 8 August 2003)

We demonstrate the control of the dispersion of matter wave packets utilizing periodic potentials. This is analogous to the technique of dispersion management known in photon optics. Matter wave packets are realized by Bose-Einstein condensates of ^{87}Rb in an optical dipole potential acting as a one-dimensional waveguide. A weak optical lattice is used to control the dispersion relation of the matter waves during the propagation of the wave packets. The dynamics are observed in position space and interpreted using the concept of effective mass. By switching from positive to negative effective mass, the dynamics can be reversed. The breakdown of the approximation of constant, as well as experimental signatures of an infinite effective mass are studied.

DOI: 10.1103/PhysRevLett.91.060402 PACS numbers: 03.75.Be, 03.75.Lm, 32.80.Pj

The broadening of particle wave packets due to the free space dispersion is one of the most prominent quantum phenomena cited in almost every textbook of quantum mechanics. The realization of Bose-Einstein condensates of dilute gases allows for the direct observation of wave packet dynamics in real space on a macroscopic scale [1]. Using periodic potentials it becomes feasible to experimentally study to what extent the matter wave dispersion relation can be engineered. This approach is similar to dispersion management for light pulses in spatially periodic refractive index structures [2].

First experiments in this direction have already been undertaken in the context of Bloch oscillations of thermal atoms [3] and condensates [4]. The modification of the dipole mode oscillation frequency of a condensate due to the changed dispersion relation in the presence of a periodic potential has been studied in detail [5,6]. In contrast to these experiments where the center of mass motion was studied, we are investigating the evolution of the spatial distribution of the atomic cloud in a quasi-one-dimensional situation. Our experiments show that the dispersion and thus the wave packet dynamics can be experimentally controlled. This is a new tool which also allows one to study the interplay between dispersion and atom-atom interaction and to realize predicted non-spreading wave packets such as gap solitons [7] and self-trapped states [8].

For atomic matter waves inside a one-dimensional optical waveguide, we have achieved dispersion management by applying a weak periodic potential with adjustable velocity. Figure 1 shows the results of an experiment in which the propagation of an atomic wave packet is studied in the normal [Fig. 1(b)] and anomalous [Fig. 1(c)] dispersion regime corresponding to positive and negative effective mass, respectively. A broadening of the wave packet is observed in both cases. The faster spreading in the case of anomalous dispersion is a consequence of the smaller absolute value of the negative effective mass. However, if we switch from one regime to the other during the propagation by changing the velocity of the periodic potential, the effects of normal and anomalous dispersion cancel. The wave packet, which has initially broadened under the influence of normal dispersion, reverses its expansion and compresses until it regains its initial shape [Fig. 1(d)]. This is a direct proof of the realization of negative effective mass.

The wave packets have been realized with a ^{87}Rb Bose-Einstein condensate. The atoms are collected in a magneto-optical trap and subsequently loaded into a

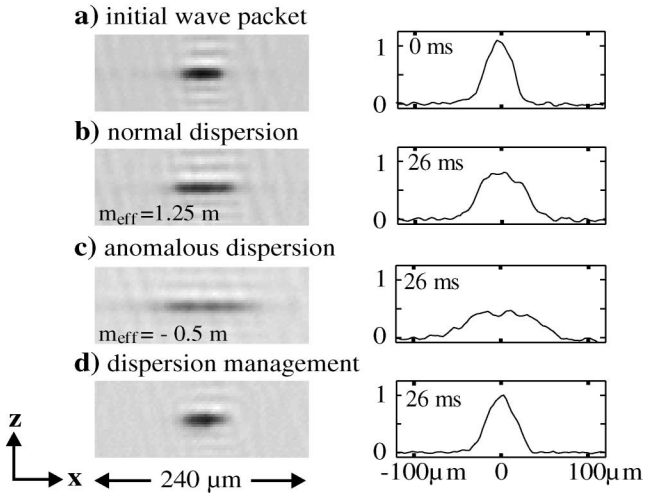

FIG. 1. Controlling the dispersion of an atomic wave packet in a waveguide using a periodic potential. Shown are absorption images of the wave packet averaged over four realizations (left) and the corresponding density distributions $n(x, t)$ along the waveguide (right). (a) Initial wave packet. (b),(c) Images taken after an overall propagation time of $t = 26$ ms for different dispersion regimes with different effective masses as indicated. (d) Wave packet subjected to dispersion management: an initial stage of expansion for $t = 17$ ms with normal dispersion is followed by propagation with anomalous dispersion for $t = 9$ ms. The broadening in the normal dispersion regime has been reversed by anomalous dispersion.

 0031-9007/03/91(6)/060402(4)$20.00

magnetic time-orbiting potential trap. By evaporative cooling we produce a cold atomic cloud which is then transferred into an optical dipole trap realized by two focused Nd:YAG laser beams with 60 μm waist crossing at the center of the magnetic trap. Further evaporative cooling is achieved by lowering the optical potential leading to pure Bose-Einstein condensates with up to 3×10^4 atoms in the $|F = 2, m_F = +2\rangle$ state. By switching off one dipole trap beam the atomic matter wave is released into a trap acting as a one-dimensional waveguide with radial trapping frequency $\omega_\perp = 2\pi \times 80\,\mathrm{Hz}$ and longitudinal trapping frequency $\omega_\parallel = 2\pi \times 1.5\,\mathrm{Hz}$.

The periodic potential is realized by a far off-resonant standing light wave with a single beam peak intensity of up to $5\,\mathrm{W/cm^2}$. The chosen detuning of 2 nm to the blue off the D2 line leads to a spontaneous emission rate below 1 Hz. The frequency and phase of the individual laser beams are controlled by acousto-optic modulators driven by a two channel arbitrary waveform generator allowing for full control of the velocity and amplitude of the periodic potential. The absolute value of the potential depth was calibrated independently by analyzing results on Bragg scattering [9] and Landau Zener tunneling [4,10].

The wave packet evolution inside the combined potential of the waveguide and the lattice is studied by taking absorption images of the atomic density distribution after a variable time delay. The density profiles along the waveguide, $n(x, t)$, are obtained by integrating the absorption images over the transverse dimension z.

The concept of effective mass m_{eff} [11] allows one to describe the dynamics of matter wave packets inside a periodic potential in a simple way via a modified dispersion relation. The periodic potential in our experiments is well described by

$$V(x) = \frac{V_0}{2}\cos(Gx)$$

with a modulation depth V_0 on the order of the grating recoil energy $E_G = \hbar^2 G^2/8m$, with $G = 2\pi/d$ where $d = 417\,\mathrm{nm}$ represents the spatial period. The energy spectrum of atoms inside the periodic potential exhibits a band structure $E_n(q)$ which is a periodic function of quasimomentum q with periodicity G corresponding to the width of the first Brillouin zone [Fig. 2(a)]. In our experiment, we prepare condensates in the lowest energy band ($n = 0$) with a quasimomentum distribution $w(q)$ centered at $q = q_c$ with an rms width $\Delta q \ll G$ [12].

It has been shown by Steel *et al.* [13] that in this case the condensate wave function in a quasi-one-dimensional situation can be described by $\Psi(x, t) = A(x, t)\ \phi_{q_c}(x) \times \exp[-iE_0(q_c)t/\hbar]$, where ϕ_{q_c} represents the Bloch function in the lowest energy band corresponding to the central quasimomentum. The evolution of the envelope function $A(x, t)$, normalized to the total number of atoms N_0, is described by

$$i\hbar\left(\frac{\partial}{\partial t} + v_g\frac{\partial}{\partial x}\right)A = -\frac{\hbar^2}{2m_{\mathrm{eff}}}\frac{\partial^2}{\partial x^2}A + \tilde{g}|A|^2A. \quad (1)$$

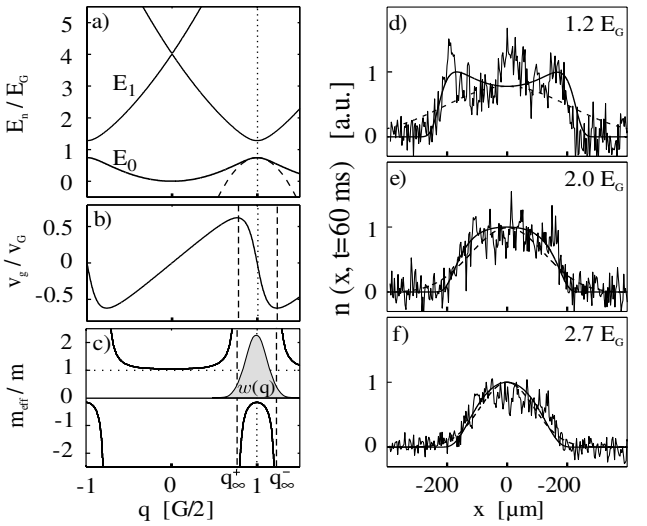

FIG. 2. (a) Band structure in the first Brillouin zone for atoms in an optical lattice with $V_0 = 1.2\,E_G$ (solid), parabolic approximation to the lowest energy band at $q = G/2$ (dashed), corresponding group velocity (b), and effective mass (c) in the lowest energy band. The vertical dashed lines at $q = q^{\pm}_{\infty}$ indicate where $|m_{\mathrm{eff}}| = \infty$. (d)–(f) Spatial densities of the wave packet after $t = 60\,\mathrm{ms}$ of propagation with $q_c = G/2$ for different V_0. The position x along the waveguide is measured in the moving frame of the optical lattice. The solid lines represent the theoretical predictions using linear propagation with the exact band structure and the quasimomentum distribution given in graph (c). The dashed lines in graphs (d)–(f) represent the prediction of the constant effective mass approximation.

The strength of the atom-atom interaction is given by $\tilde{g} = \alpha_{nl} 2\hbar\omega_\perp a$, with the s-wave scattering length a, and a renormalization factor $\alpha_{nl} = (1/d)\int_0^d dx|\phi_{q_c}|^4$. Besides the modification of the nonlinear term the periodic potential leads to a group velocity of the envelope $A(x, t)$ determined by the energy band via $v_g(q_c) = \hbar^{-1}[\partial E_0(q)/\partial q]|_{q_c}$ [Fig. 2(b)]. In addition, the kinetic energy term describing the dispersion of the wave packet is modified by the effective mass [Fig. 2(c)]

$$m_{\mathrm{eff}}(q_c) = \hbar^2\left[\frac{\partial^2 E_0(q)}{\partial q^2}\bigg|_{q_c}\right]^{-1}.$$

Since this approximation of constant effective mass corresponds to a parabolic approximation of the energy band, it is valid only for sufficiently small Δq.

The general solution of Eq. (1) is a difficult task, but simple analytic expressions can be found in the special cases of negligible and dominating atom-atom interaction. Omitting the last term in Eq. (1) it is straightforward to see that $|m_{\mathrm{eff}}|$ controls the magnitude of the dispersion term and thus the time scale of the wave packet broadening. A change in sign of m_{eff} corresponds to time reversal of the dynamics in a frame moving with velocity v_g. In the regime where the atom-atom interaction is dominating, e.g., during the initial expansion of a condensate, the evolution of the envelope function can be

found in standard nonlinear optics textbooks [2] and in the form of scaling solutions in the context of Bose-Einstein condensates [14]. Note that in this regime the kinetic energy term is still relevant and thus a change of the sign of the effective mass will reverse the dynamics.

In the following we will analyze the obtained experimental results in more detail. The initial wave packet shown in Fig. 1(a) contains 2×10^4 atoms and is characterized by $\Delta x_0 = 14.8(6)\,\mu$m ($\Delta x$ is the rms width of a Gaussian fit). Before releasing the atomic cloud into the one-dimensional waveguide, a weak periodic potential along the waveguide is adiabatically ramped up to $V_0 = 2.8(2)\,E_G$ within 6 ms. This turns the initial Gaussian momentum distribution of the atoms into a Gaussian distribution of quasimomenta $w(q)$ centered at $q_c = 0$ with a corresponding effective mass $m_{\text{eff}} = 1.25\,m$. The density distribution shown in Fig. 1(b) is a result of propagation within the stationary periodic potential for $t = 26$ ms and exhibits a spread of $\delta x := \sqrt{\Delta x(t)^2 - \Delta x_0^2} = 18.4(12)\,\mu$m in contrast to $\delta x_f = 20.2(14)\,\mu$m for expansion without periodic potential. The resulting ratio $\delta x_f/\delta x = 1.10(15)$ indicates that the evolution is dominated by the nonlinearity, in which case one expects $\delta x_f/\delta x \approx \sqrt{m_{\text{eff}}/m} = 1.11$ in the short-time limit [15]. In the case of linear propagation one expects $\delta x_f/\delta x = m_{\text{eff}}/m = 1.25$.

The dynamics in the anomalous dispersion regime [Fig. 1(c)] are investigated by initially accelerating the periodic potential within 3 ms to a velocity $v = v_G := \hbar G/2m$, thus preparing the atomic wave packet at the edge of the Brillouin zone ($q_c = G/2$), where $m_{\text{eff}} = -0.5\,m$. The velocity is kept constant during the subsequent expansion. In the regime of negative mass a condensate exhibits collapse dynamics. Two-dimensional calculations for our experimental situation reveal that this collapse happens within the initial 3–6 ms of propagation. Subsequently this leads to an excitation of transverse states and thus to a fast reduction of the density and the nonlinearity. An indication of the population of transverse states is the observed increase of the transverse spatial extension of the wave packets by almost a factor of 2. The optical resolution of our setup does not allow for a quantitative analysis of the transverse broadening. Because of the fast reduction of the nonlinearity the subsequent expansion should be well described by linear theory predicting a ratio $\delta x_f/\delta x = 0.5$ which is close to the observed value 0.46(5) [$\delta x = 38.5(15)\,\mu$m after 23 ms].

In the case of dispersion management Fig. 1(d) the wave packet was first subjected to normal dispersion for 17 ms at $q_c = 0$. The time of subsequent propagation with anomalous dispersion at $q_c = G/2$ was adjusted to achieve the minimal wave packet size of $\Delta x = 15.4(2)\,\mu$m. The minimum was achieved for times ranging from 7 to 9 ms which is in rough agreement with the expected time resulting from effective mass considerations $\sqrt{0.5/1.25} \times 17\,\text{ms} = 10.7\,\text{ms}$.

Since the assumption of a constant effective mass used so far is only an approximation, it is important to check its applicability in experiments. Therefore we investigate the dynamics of wave packets prepared at the Brillouin zone edge for different potential depths. The observed density profiles after 60 ms of propagation are shown in Figs. 2(d)–2(f). While both the initial wave packet shape $n(x, 0)$ and the quasimomentum distribution $w(q)$ are measured to be approximately Gaussian, the wave packet changes its shape during evolution. We attribute this distortion to the invalidity of the constant effective mass approximation, which assumes that the populated quasimomenta experience the same negative curvature of $E_0(q)$. Since the range of quasimomenta fulfilling this criterion becomes smaller with decreasing modulation depth, a more pronounced distortion of the wave packet shape for weak potentials is expected [see Fig. 2(d)].

This explanation is confirmed more quantitatively by comparing the observed wave packets with the results of a linear theory. Since the initial collapse of the condensate cannot be described by a linear theory, we take a Gaussian function fitted to the density distribution measured at 20 ms as the initial wave packet for the numerical propagation. Because of the fact that this is not a minimum uncertainty wave packet we add a quadratic phase in real space such that the Fourier transform of the wave packet is consistent with the measured momentum distribution. In first approximation this takes into account the initial expansion including the repulsive atom-atom interaction. For the subsequent propagation of 40 ms in quasimomentum space we use the full expression for $E_0(q)$ which is obtained numerically. In Fig. 2(d)–2(f) we compare the data with the linear theory described above (solid line) and with the constant effective mass approximation (dashed line). Clearly the constant effective mass approximation cannot explain the observed distortion and it strongly overestimates the expansion velocity for weak potentials. Additionally, for small potential modulation depths new features appear in the central part of the wave packet which cannot be explained using the linear theory. We are currently investigating these features in more detail.

The observed distortion is mainly a consequence of another very interesting feature of the band structure: the existence of $|m_{\text{eff}}| = \infty$ for certain quasimomenta $q = q_\infty^\pm$ [see Fig. 2(c)]. A diverging mass implies that the group velocity is extremal and the dispersion vanishes as can be seen from Eq. (1). As a consequence an atomic ensemble whose quasimomentum distribution is overlapping $q = q_\infty^\pm$ will develop steep edges as can be seen in Fig. 2(d) and in Fig. 3. These edges propagate with the maximum group velocity of the lowest band.

The systematic investigation of the velocities of the edges is shown in Fig. 3 for different values of V_0. In order to get a significant overlap of $w(q)$ with $q = q_\infty^\pm$, we

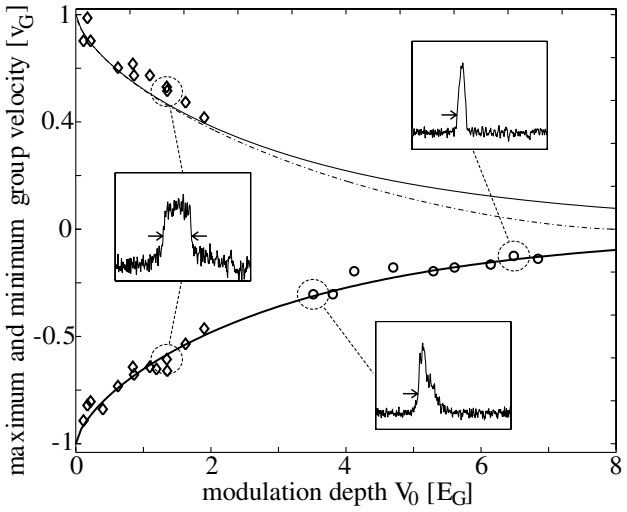

FIG. 3. Group velocities of steep edges emerging from an initial wave packet with significant overlap with $q_\infty^{\pm}$ in quasimomentum space. The measured velocities of the indicated positions (arrows in insets) agree very well with the expected maximum and minimum velocity in the lowest band (solid line) corresponding to the infinite masses. The dashed line represents the prediction of the weak potential approximation [11]. For potentials smaller than $2\,E_G$ (diamonds) data are obtained by preparing the initial wave packet at $q = G/2$ leading to two steep edges (see inset). For higher potentials (circles) the wave packet is prepared at $q = G/4$ to ensure population of the quasimomentum corresponding to infinite mass.

prepare atomic ensembles with $\Delta q = 0.17\,G/2$ at $q_c = G/2$ realized by Bose-Einstein condensates of 2×10^4 atoms with a spatial extension of $\Delta x = 15\,\mu$m. The velocities of the edges are derived from two images taken at 20 and 60 ms, respectively. In each image the position of the edge is evaluated at the levels indicated by the arrows in the insets of Fig. 3 (50% and 25% of the maximum density). Since the momentum spread is too small to populate the infinite mass points for potentials deeper than $2\,E_G$ the atomic ensemble was then prepared at $q_c = G/4$. The resulting wave packet shapes are asymmetric exhibiting a steep edge on one side which becomes less pronounced for potentials deeper than $5\,E_G$. The obtained experimental results in Fig. 3 are in excellent agreement with the numerically calculated band structure predictions. In contrast to the good agreement of the maximum velocity for all potential depths we find that for $V_0 > 5\,E_G$ the group velocity of the center of mass is only 10% of the expected velocity. This could be an indication of entering the tight binding regime where the nonlinear effect of self-trapping, i.e., stopping and nonspreading wave packets, has been predicted [8]. We are currently investigating the transport properties in this regime in more detail.

In conclusion, we have demonstrated experimentally that the dispersion of atomic matter waves in a waveguide can be controlled using a weak periodic potential. Matter wave packets with positive, negative, and infinite effective masses are studied in the regime of weak and intermediate potential heights. The preparation of matter waves with engineered dispersion ($m_{\text{eff}} < 0$) is an important prerequisite for the experimental investigation of atomic gap solitons and other effects arising from the coherent interplay of nonlinearity and dispersion in periodic potentials.

We wish to thank J. Mlynek for his generous support, A. Sizmann and B. Brezger for many stimulating discussions, and J. Bellanca and K. Forberich for their help in building up the experiment. This work was supported by Deutsche Forschungsgemeinschaft, Emmy Noether Program, and by the European Union, Contract No. HPRN-CT-2000-00125.

Note added.—Only recently, we became aware of an experimental work [16] which is closely related to the work presented in this Letter.

[1] *Bose-Einstein Condensation in Atomic Gases*, edited by M. Inguscio, S. Stringari, and C. Wieman (IOS Press, Amsterdam, 1999).
[2] G. P. Agrawal, *Applications of Nonlinear Fiber Optics* (Academic Press, San Diego, 2001); *Nonlinear Fiber Optics* (Academic Press, San Diego, 1995).
[3] M. Ben Dahan, E. Peik, J. Reichel, Y. Castin, and C. Salomon, Phys. Rev. Lett. **76**, 4508 (1996).
[4] B. P. Anderson and M. A. Kasevich, Science **282**, 1686 (1998); O. Morsch, J. Müller, M. Cristiani, D. Ciampini, and E. Arimondo, Phys. Rev. Lett. **87**, 140402 (2001).
[5] S. Burger, F. S. Cataliotti, C. Fort, F. Minardi, M. Inguscio, M. L. Chiofalo, and M. P. Tosi, Phys. Rev. Lett. **86**, 4447 (2001).
[6] M. Krämer, L. Pitaevskii, and S. Stringari, Phys. Rev. Lett. **88**, 180404 (2002).
[7] P. Meystre, *Atom Optics* (Springer-Verlag, New York, 2001), p. 205, and references therein.
[8] A. Trombettoni and A. Smerzi, Phys. Rev. Lett. **86**, 2353 (2001).
[9] M. Kozuma, L. Deng, E. W. Hagley, J. Wen, R. Lutwak, K. Helmerson, S. L. Rolston, and W. D. Phillips, Phys. Rev. Lett. **82**, 871 (1999).
[10] C. F. Bharucha, K. W. Madison, P. R. Morrow, S. R. Wilkinson, Bala Sundaram, and M. G. Raizen, Phys. Rev. A **55**, R857 (1997).
[11] N. Ashcroft and N. Mermin, *Solid State Physics* (Saunders, Philadelphia, 1976).
[12] J. Hecker-Denschlag, J. E. Simsarian, H. Häffner, C. McKenzie, A. Browaeys, D. Cho, K. Helmerson, S. L. Rolston, and W. D. Phillips, J. Phys. B **35**, 3095 (2002), and references therein.
[13] M. Steel and W. Zhang, cond-mat/9810284.
[14] Y. Castin, and R. Dum, Phys. Rev. Lett. **77**, 5315 (1996); Yu. Kagan, E. L. Surkov, and G. V. Shlyapnikov, Phys. Rev. A **54**, R1753 (1996).
[15] M. J. Potasek, G. P. Agrawal, and S. C. Pinault, J. Opt. Soc. Am. B **3**, 205 (1986).
[16] L. Fallani, F. S. Cataliotti, J. Catani, C. Fort, M. Modugno, M. Zawada, and M. Inguscio, cond-mat/0303626.